

# Lack of Ultrametricity in the Low Temperature phase of 3D Ising Spin Glasses

Guy Hed

Department of Materials and Interfaces, Weizmann Institute of Science, Rehovot 76100, Israel

A. P. Young

Department of Physics, University of California, Santa Cruz, CA 95064

Eytan Domany

Department of Physics of Complex Systems, Weizmann Institute of Science, Rehovot 76100, Israel

We study the low-temperature spin-glass phases of the Sherrington-Kirkpatrick (SK) model and of the 3-dimensional short range Ising spin glass. For the SK model, evidence for ultrametricity becomes clearer as the system's size increases, while for the short-range case our results indicate the opposite, i.e. lack of ultrametricity. Our results are obtained by two methods: a recently proposed one that uses clustering to focus on the relevant parts of phase space and reduce finite size effects, and another method which does not rely on clustering.

The mean-field solution of Ising spin glasses (ISG), known to be exact for the Sherrington-Kirkpatrick (SK) model [1], exhibits a non-trivial low-temperature phase [2]. One of the central open questions of the field is whether the qualitative structure of the mean-field solution is valid also for 3-dimensional short-range Ising Spin Glasses (3dISG). Both systems are described by the N-spin Hamiltonian

$$H(\mathbf{s}) = \sum_{\langle i,j \rangle} J_{ij} s_i s_j; \quad (1)$$

where  $s_i = \pm 1$ . In the SK model the sum in Eq. (1) runs over all pairs of spins, while in the 3dISG the sum is over nearest neighbor sites of a cubic lattice. The interactions  $J_{ij}$  are taken from a Gaussian distribution with mean zero and variance  $1/(N-1)$  in the SK model, while the variance is 1 for the 3dISG.

To test the validity of the mean-field solution, it is natural to consider first the most widely calculated observable in ISG; the distribution  $P(q)$  of the overlaps  $q$ , defined for two states  $\mathbf{s}$  and  $\mathbf{s}'$  as  $q = N^{-1} \sum_{i=1}^N s_i s'_i$ . For each realization of the randomly selected  $J_{ij}$  one calculates the probability distribution  $P_J(q)$  (at equilibrium at some temperature);  $P(q) = \langle P_J(q) \rangle_{\text{av}}$  is the average over the different realizations of the disorder. Indeed,  $P(q)$  was measured by Monte-Carlo simulations [3] and in other ways [4, 5] and non-trivial overlap distributions were found for both the SK and 3dISG. However, there were clear indications that the nature of the low T phases of the two models were different [6, 7]. In particular, evidence was presented [7] for lack of ultrametricity in 3dISG.

Ultrametricity (UM) of the state space [8] is one of the main characteristics of the low T phase of the mean-field solution and the SK model. Consider an equilibrium ensemble of microstates at  $T < T_c$ , and pick three,  $\mathbf{s}, \mathbf{s}',$  and  $\mathbf{s}''$  at random (see, however, point (a) below). These indices represent the states  $\mathbf{s}, \mathbf{s}'$  and  $\mathbf{s}''$ . Order them so

that  $q_{\mathbf{s}\mathbf{s}'} \geq q_{\mathbf{s}\mathbf{s}''} \geq q_{\mathbf{s}'\mathbf{s}''}$ ; ultrametricity means that in the thermodynamic limit we get  $q_{\mathbf{s}\mathbf{s}'} = q_{\mathbf{s}\mathbf{s}''}$  with probability 1. In terms of the distances  $d_{\mathbf{s}\mathbf{s}'} = (1 - q_{\mathbf{s}\mathbf{s}'})/2$  the condition of UM becomes  $d_{\mathbf{s}\mathbf{s}'} = d_{\mathbf{s}\mathbf{s}''} = d_{\mathbf{s}'\mathbf{s}''}$ .

Even though claims were made for the emergence of UM for large 3D systems [9], these were not conclusive. Since demonstrating lack of ultrametricity suffices to prove that the mean-field solution does not apply for the 3dISG, the evidence presented in [7] prompted Chiliberti and Marinari (CM) [10] to use similar methods at the same system sizes as used by [7], to search for ultrametricity in the SK model, which has an ultrametric low-T phase. CM did not see UM in the SK model and claimed that the system sizes used were too small to allow observation of ultrametricity. CM argued further that failure to see UM where it holds indicates that similar failure reported [7] for the 3dISG does not provide evidence for its absence.

In order to settle this issue we performed extensive simulations of the SK model for a somewhat larger range of sizes than in CM, and carried out a careful analysis of the results. We also applied the same method of analysis to our earlier [7] results for the 3dISG model. As opposed to CM, we found clear evidence for UM in the SK model; its signature becomes more pronounced as the system size increases. On the other hand, for the 3dISG we found the opposite; with increasing system size the results become less consistent with UM. We will explain in detail elsewhere [11] the reasons for the differences between our results and those of CM. Here we note that in order to observe UM one has to avoid three main pitfalls:

- If time reversal symmetry is unbroken (zero magnetic field), the phase space structure consists of two spin- $\mathbb{Z}_2$  related pure-state hierarchies (see Fig. 1). UM can be observed only if all three states of each sampled triplet belong to the same side [12].
- Do not work too close to  $T_c$ ; finite size effects mask the signal.

(c) At low  $T$ , most of the microstates belong to the same pure state [8]. With increasing  $N$  the overlaps inside a pure state converge to  $q_{EA}$  and most  $f_j$ ;  $g_j$  triangles become equilateral, conveying no information on UM.

Pitfalls (a) and (c) require special care when choosing the triangles of states for which UM is tested. First, we map out the upper levels of the pure state hierarchy by clustering [7, 13] (see Fig 1). To avoid (a), we consider only triplets of states from (say) the left tree. To avoid (c) we pick the three states from different pure states of this tree.

Monte Carlo simulations: SK systems were simulated at sizes  $N = 32; 128; 256; 1024$ . To speed up equilibration we used parallel tempering [14, 15], with 21 temperatures ranging from 2.0 down to 0.2. For the largest size,  $N = 1024$ , we performed 450,000 sweeps for each set of spins, with measurements being carried out during the last 300,000 sweeps. Tests for equilibration were carried out as in Ref. 6. Details of the simulations on the 3dISG are given in Ref. 7. For each size we generated 500 different realizations  $f_j g_j$  of the disorder (except for  $N = 8^3$  - only 335 realizations). For each  $f_j g_j$  we generated 500 microstates, sampled according to the Boltzmann distribution at  $T = 0.2$ . Each sample of states was enhanced to 1000 by adding to these 500 microstates their spin-inverted images. The result is two spin-inverted unbiased samples - one from each tree. The microstates appear in the random order generated by the Monte Carlo procedure.

Identification of pure states by clustering: The 1000 microstates, obtained for a realization of the disorder  $f_j g_j$  occupy 1000 corners of an  $N$ -dimensional hypercube. We assign these 1000 points to groups and determine their relative tree-like structure [7] by clustering. Here [16] we used the well known average linkage agglomerative clustering algorithm [17]. Initially each of the  $M = 1000$  points (microstates) is a cluster; at every clustering step those two clusters that are closest are merged to form a new cluster; the process stops after  $M - 1$  steps when all the points belong to one cluster. The distance  $d_{ij}$  between clusters is defined as the average distance between points of  $i$  and  $j$ . After every merging operation we record for the new cluster  $k = [i, j]$  the score  $s_k = d_{ij}$ , and for each of the merged clusters a quality measure  $v_k = s_i s_j$ . If  $v_k$  is high, the distances between states within  $k$  are significantly smaller than the distances of these states from states outside  $k$ , and cluster  $k$  is "real", i.e. not an artifact of the agglomerative procedure.

Fig. 1 presents the tree of clusters (dendrogram) obtained when the procedure outlined above was applied to the equilibrium ensemble of 1000 microstates, obtained at  $T = 0.2$  for a particular realization  $f_j g_j$  of the SK model with  $N = 1024$  spins. The clusters at the higher levels of the hierarchy have high  $v$  values, suggesting

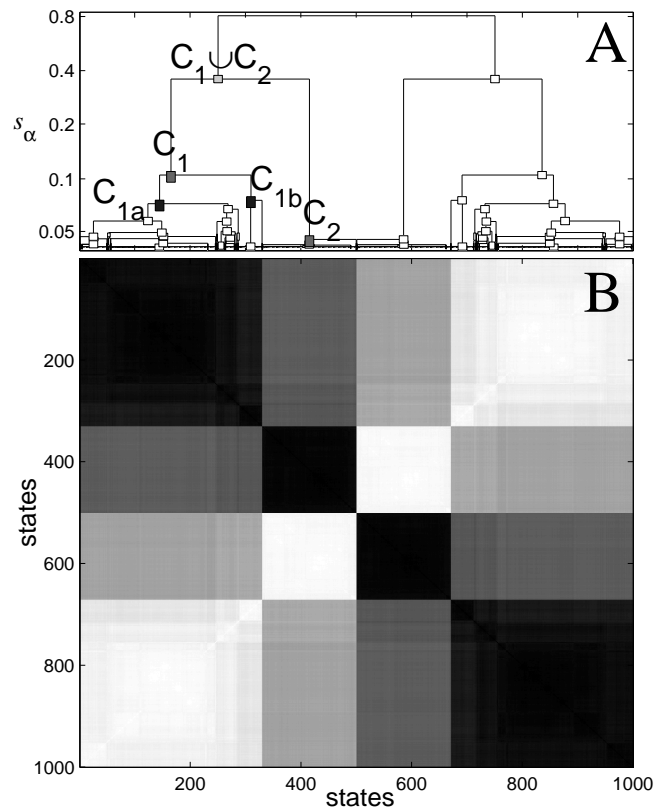


FIG. 1: (A) Clustering produces the dendrogram of state clusters, for the equilibrium ensemble of 1000 states, obtained by simulation of one realization of the SK model for 1024 spins, at  $T = 0.2$ . The vertical position of each cluster is its score  $s$ . Logarithmic scale is used for the vertical axis; only clusters with  $s > 0.04$  are shown. Significant clusters, identified by a long branch above them, have high values of  $v$ ; these clusters reflect presence of dense regions in the underlying Boltzmann distribution. (B) The distance matrix  $d$  of the microstates, that were reordered according to their positions, as the leaves of the dendrogram, on the horizontal axis of (A). Darker colors indicate smaller distances.

that the partitions they form indeed exist in the underlying distribution from which the states were taken. That is, they map the microstates in our sample to the pure states from which they were taken.

At the highest level, the dendrogram splits into two identical trees, which are the two spin-inverted pure state trees. We consider the states that belong to one (the left). For all  $f_j g_j$  we call the two top level state clusters by  $C_1$  and  $C_2$  with the convention  $f_{1j} g_{1j}$ ;  $f_{2j} g_{2j}$ . The two subclusters of  $C_1$  are denoted by  $C_{1a}$  and  $C_{1b}$ . The triplets of microstates for which we test UM are selected as follows:  $2 C_{1a}$ ,  $2 C_{1b}$  and  $2 C_2$ . If state space is ultrametric and these clusters correspond to the underlying pure states, we expect  $d = d \quad d$ .

Direct Measurement of Ultrametricity: For each triplet of states  $i, j, k$  and selected as described above, we define

3dISG			SK			Naive SK	
N	$\overline{K}$	P(K = 1)	N	$\overline{K}$	P(K = 1)	$\overline{K}$	P(K = 1)
4 <sup>3</sup>	0.357 (12)	0.617 (16)	32	0.331 (9)	0.350 (16)	0.316 (6)	0.759 (7)
5 <sup>3</sup>	0.576 (12)	0.233 (13)	128	0.346 (8)	0.037 (5)	0.405 (4)	0.365 (7)
6 <sup>3</sup>	0.548 (10)	0.144 (9)	256	0.294 (7)	0.005 (1)	0.423 (3)	0.127 (4)
8 <sup>3</sup>	0.502 (12)	0.044 (5)	512	0.236 (6)	5 (3) 10 <sup>-4</sup>	0.395 (2)	0.015 (1)
			1024	0.182 (5)	2 (1) 10 <sup>-6</sup>	0.345 (3)	1.8 (2) 10 <sup>-4</sup>

TABLE I: The values of  $\overline{K}$  as a function of N, for both the SK and 3dISG. See text for definitions.

an index [7]

$$K = \frac{\sum_i d_j}{d} \quad (2)$$

Note that  $0 \leq K \leq 1$  due to the triangle inequality.

For a given realization  $fJg$  we identify  $C_{1a}$ ,  $C_{1b}$ , and  $C_2$ , and measure  $K$  over all the corresponding state triplets. We discard triplets with  $K = 1$  since these correspond to co-linear "triangles" (they are the result of a finite size effect, and their weight  $P(K = 1)$  decreases rapidly with increasing system size, as seen in Table I. We calculate the distribution  $P_J(K) = P_J(K = K | K < 1)$ , and its mean  $\overline{K}_J$ . We then average over the realizations  $fJg$  to get  $\overline{K} = \langle \overline{K}_J \rangle_{\text{av}}$  and  $P(K) = \langle P_J(K) \rangle_{\text{av}}$ . If state space is UM in the thermodynamic limit, we expect  $\overline{K} \rightarrow 0$  and  $P(K) \rightarrow \delta(K)$  as  $N \rightarrow \infty$ .

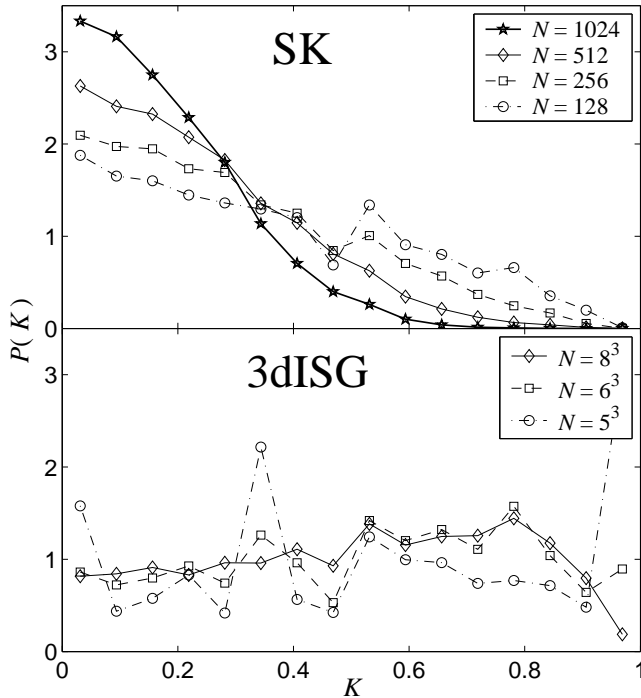


FIG. 2: The distributions  $P(K)$  (see text), calculated for 3dISG and SK systems for various sizes N.

We present in Fig. 2 the distributions  $P(K)$  obtained for a sequence of sizes N for the SK and 3dISG models. For the SK model the peak of  $P(K)$  is at  $K = 0$  and its width decreases as N increases, as expected if  $P(K)$  is to approach  $\delta(K)$ . The behavior is markedly different for the 3dISG: the width of the distribution remains constant and its peak is at  $K \approx 0.3$ . For the SK model the values of  $\overline{K}$ , presented in Table I, are smaller, decrease faster and approach zero as N increases, whereas for the 3dISG  $\overline{K}$  seems to go to a non-vanishing limiting value. For both systems the lowest size is useless for estimating the trend with increasing N.

We present also the results obtained for the SK model by a "naive" calculation, that neglects to ensure that all members of a triplet of states are drawn from the same side of the dendrogram; clearly, such oversight indeed renders UM unobservable [10].

Another test of UM is the following: if the state space is ultrametric, then the distance between states  $\in C_1$  and  $\in C_2$  depends only on the identity of their closest common ancestor on the tree of pure states, which is  $C_1 \cap C_2$ . Thus, for each realization, the sub-matrix  $q_{C_1 C_2}$  should be uniform (e.g. the rectangle in the distance matrix of Fig. 1, that connects states from  $C_1$  and  $C_2$ , should be uniformly shaded).

We have calculated the standard deviation  $s_{C_1 C_2}$  and the average  $\langle q_{C_1 C_2} \rangle$  of the elements of  $q_{C_1 C_2}$  for each realization  $fJg$ . For a given average  $\langle q_{C_1 C_2} \rangle$  the standard deviation is bounded by  $\sqrt{\langle q_{C_1 C_2} \rangle (1 - \langle q_{C_1 C_2} \rangle)}$  – the standard deviation of a Bernoulli distribution. We define a normalized standard

3dISG			SK		
N	$\langle q_{C_1 C_2} \rangle_{\text{av}}$	$s_{C_1 C_2} / \langle q_{C_1 C_2} \rangle_{\text{av}}$	N	$\langle q_{C_1 C_2} \rangle_{\text{av}}$	$s_{C_1 C_2} / \langle q_{C_1 C_2} \rangle_{\text{av}}$
4 <sup>3</sup>	0.050 (2)	0.135 (7)	32	0.098 (3)	0.338 (29)
5 <sup>3</sup>	0.045 (2)	0.123 (6)	128	0.064 (2)	0.196 (12)
6 <sup>3</sup>	0.043 (2)	0.133 (10)	256	0.054 (2)	0.170 (10)
8 <sup>3</sup>	0.042 (2)	0.136 (9)	512	0.043 (1)	0.142 (10)
			1024	0.034 (1)	0.115 (10)

TABLE II: The standard deviation  $s_{C_1 C_2}$  and the normalized standard deviation  $S_{C_1 C_2}$  of the elements of  $q_{C_1 C_2}$  (see text), averaged over realizations of the disorder  $fJg$ , for 3dISG and SK systems of different sizes.

deviation  $S_{C_1 C_2} = s_{C_1 C_2} = \frac{1}{m_{C_1 C_2}} \sqrt{\frac{1}{m_{C_1 C_2}} \sum_{i=1}^{m_{C_1 C_2}} (1 - m_{C_1 C_2})}$ . We average over the realizations to get  $[S_{C_1 C_2}]_{\text{av}}$  and  $[s_{C_1 C_2}]_{\text{av}}$ . The results are given in Table II. For the SK model both  $[S_{C_1 C_2}]_{\text{av}}$  and  $[s_{C_1 C_2}]_{\text{av}}$  decrease rapidly as  $N$  increases, indicating again that UM is approached, while for the 3dISG the values of  $[S_{C_1 C_2}]_{\text{av}}$  and  $[s_{C_1 C_2}]_{\text{av}}$  seem to asymptote to 0.04 and 0.13 respectively.

Testing UM without clustering the states: We give here another way to detect UM, for which a knowledge of  $P_J(q)$  success and clustering methods are not required.

Mézard et al. [8] describe how UM is manifest in various multi-overlap distributions over the realizations  $\{J_{ij}\}$ . One of these consequences has the form

$$P_J(q_1)P_J(q_2)_{\text{av}} = \frac{2}{3}P(q_1)P(q_2) + \frac{1}{3}P(q_1)(q_1 - q_2) : \quad (3)$$

In order to test the validity of Eq. (3) we define

$$dp(q_1; q_2) = \frac{3P_J(q_1)P_J(q_2)_{\text{av}} - 2P(q_1)P(q_2)}{P(q_1)} : \quad (4)$$

If state space is UM, then  $dp(q_1; q_2)$  converges [18] to  $(q_1 - q_2)$  as  $N \rightarrow \infty$ . Fig. 3 presents  $dp$  versus  $|q_1 - q_2|$ . For the SK model  $dp$  approaches  $(q_1 - q_2)$  with increasing  $N$ , as expected if UM is to hold. However, for the 3dISG the height of the peak at 0 decreases and seems to converge to a finite value, and the width remains constant.

We also examined the equality of the second moment of Eq. (3):  $[dp^2]_{\text{av}} = \frac{2}{3}[dp^2]_{\text{av}} + \frac{1}{3}[dp^4]_{\text{av}}$ , which has been investigated numerically in other work [19]. We find that the ratio of the two sides is one for all systems

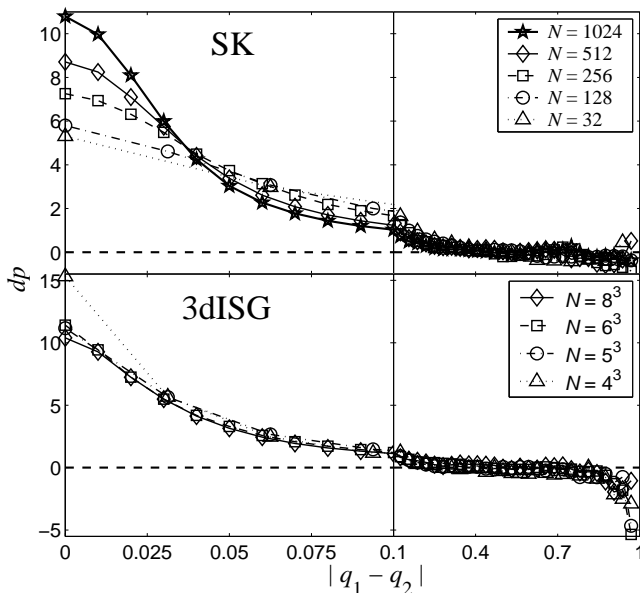


FIG. 3: The distribution of  $dp(q_1; q_2)$  averaged over overlap pairs  $\{q_1; q_2\}$  with the same difference  $|q_1 - q_2|$ .

examined within an error smaller than 0.03, in agreement with Ref. 19. However, moments may be insensitive to deviations from UM because  $dp \rightarrow 0$  when  $|q_1 - q_2| > 0.2$ .

We presented strong evidence for the lack of UM in the low  $T$  phase of the 3-dimensional short range Ising spin glass. Several indicators of UM were tested; while for the 3dISG they consistently point to lack of UM, for SK models of similar sizes all the results strongly indicate the existence of UM. We conclude that our methods are able to detect UM, where it exists, at the system sizes studied. Our findings indicate that the structure of the low-temperature phase of spin glasses that emerges from the mean-field solution is not valid for the 3-dimensional short range Ising spin glass.

This work was supported by grants from the Ministero della Sanità and the European Community's Human Potential Programme under contract HPRN-CT-2002-00319, STIPCO. The work of APY was supported by NSF grant DMR 0086287.

- [1] D. Sherrington and S. Kirkpatrick, Phys. Rev. Lett. 35, 1792 (1975).
- [2] G. Parisi, M. Mézard, and M. A. Virasoro, Spin glass theory and beyond (World Scientific, Singapore, 1987).
- [3] E. Marinari, G. Parisi, and J. J. Ruiz-Lorenzo, Phys. Rev. B 58, 852 (1998).
- [4] F. Krzakala and O. Zeitouni, Phys. Rev. Lett. 85, 3013 (2000).
- [5] M. Palassini and A. P. Young, Phys. Rev. Lett. 85, 3017 (2000).
- [6] H. G. Katzgraber, M. Palassini, and A. P. Young, Phys. Rev. B 63, 184422 (2001).
- [7] E. Domany, G. Hed, M. Palassini, and A. P. Young, Phys. Rev. B 64, 224406 (2001).
- [8] M. Mézard, G. Parisi, N. Sourlas, G. Toulouse, and M. A. Virasoro, J. Phys. 45, 843 (1984).
- [9] S. Franz and F. Ricci-Tersenghi, Phys. Rev. E 61, 1121 (2000).
- [10] S. Ciliberti and E. Marinari, cond-mat/0304273.
- [11] G. Hed, E. Domany, and A. P. Young, to be published.
- [12] M. Mézard, private communication.
- [13] G. Hed, A. K. Hartmann, D. Stauffer, and E. Domany, Phys. Rev. Lett. 86, 3148 (2001).
- [14] K. Hukushima and K. Nemoto, J. Phys. Soc. Japan 65, 1604 (1996).
- [15] E. Marinari, in Advances in Computer Simulation, edited by J. Kertesz and I. Kondor (Springer-Verlag, 1998), p. 50, (cond-mat/9612010).
- [16] In Ref. 7 we used Ward's clustering method, which tends to ignore pure states with small statistical weight. The present scheme is more suitable for our data, but the results of the analysis are similar for both schemes.
- [17] A. K. Jain and R. C. Dubes, Algorithms for Clustering Data (Prentice-Hall, Englewood Cliffs, 1988).
- [18] Note that for a finite system  $dp(q_1; q_2)$  is not invariant under the exchange of  $q_1$  and  $q_2$ .
- [19] E. Marinari, G. Parisi, J. Ruiz-Lorenzo, and F. Ritort, Phys. Rev. Lett. 76, 843 (1996).